

# Investigations on the Experimental Setup for Testing the Centric Tensile Strength According to ASTM C307 of Mineral-based Materials

Annette Dahlhoff\*, Bernd Winkels, Cynthia Morales Cruz, Michael Raupach

*Institute of Building Materials Research (IBAC), RWTH Aachen University, Schinkelstr. 3, 52062 Aachen, Germany*

*E-mail: dahlhoff@ibac.rwth-aachen.de (Corresponding author); winkels@ibac.rwth-aachen.de; morales@ibac.rwth-aachen.de; raupach@ibac.rwth-aachen.de*

Received: 22 July 2022; Accepted: 14 September 2022; Available online: 5 November 2022

**Abstract:** Centric tensile tests often exhibit high standard deviations due to various factors, hence various test setups have been developed in the past. Based on the specifications in ASTM C307-18, the experimental setup was further developed to reduce the standard deviation resulting from the test setup itself and thus to obtain reliable, reproducible test results. Furthermore, it has been investigated, whether the test setup is suitable for materials of low strength. In the further developed experimental setup three mineral-based materials with tensile strengths in the range of 0.4 to 5.9 MPa were examined and compared to ASTM C307-18. For this purpose, the optical 3D-measurement system ARAMIS® and a positioning adapter designed for the specimen geometry were used to validate and verify the developed experimental setup and to ensure a consistent position of the specimen. For the low strength mineral-based materials tensile strength tests could be implemented and recommendations for the test parameters test speed, preload and required number of specimens could be developed.

**Keywords:** Tensile strength test; Tensile strength; DIC; Mortar; Autoclaved aerated concrete.

## 1. Introduction

The tensile load-bearing and deformation behavior of mineral-based materials can be decisive, for example, when evaluating crack resistance in the case of structural movements due to thermal expansion. There are direct and indirect tests to determine the tensile load-bearing behavior of building materials, cf. [1,2]. The test setups differ in the type of load introduction. Indirect test methods such as flexural tensile tests and splitting tensile tests result in an inhomogeneous stress distribution across the cross-section, while direct tests enable a uniform stress distribution due to axial load application. According to [3], the test methods for testing the centric tensile strength presented in [4] can be divided into four subgroups:

- 1) Load application via interlocking with test specimens of customized geometry;
- 2) Load application via steel bars embedded in the test specimen;
- 3) Lateral load application with constant or variable contact pressure;
- 4) Load application via adhered steel stamps.

The different subgroups of possible support types for load application and specimen geometry for centric tensile strength testing is shown exemplarily in Figure 1, adapted from [4].

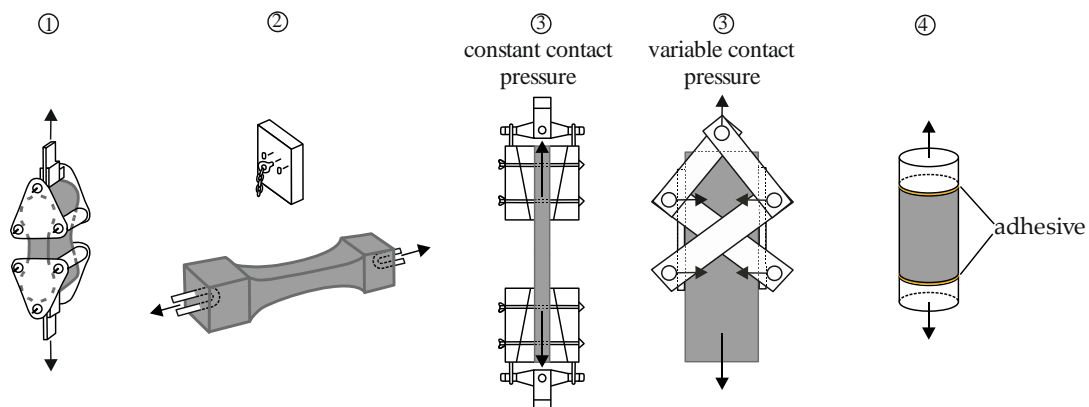


**Figure 1.** Support types for centric tensile tests adapted from [4].

Generally, a distinction is made between mechanical and bonded supports. Mechanical supports can be designed as a clamping device in which the tensile force is introduced into the specimen via lateral positive locking, or can be embedded in the test specimen, cf. Figure 1, (1) and (2). Lateral supports enable constant or variable contact pressure, cf. Figure 1, (3). In case of bonded supports, usually steel stamps are adhered to cylindrical specimen surfaces, cf. Figure 1, (4). Depending on the applied test setup, however, axial tests for example may be influenced by eccentricities, leading to an inhomogeneous stress distribution across the cross-section and thus to large scatter. Eccentricities for example can result from tilting of the steel stamps due to improper grinding or improper use of the adhesive, cf. [1]. In addition, tests at high temperatures, for example, can only be carried out with special adhesives. A major disadvantage of the centric load application by means of mechanical supports is the stress distribution at the transition zones, which can lead to premature failure in these zones and thus to high deviations [2,4]. However, centric tensile strength testing is often subject to uncertainties which, in addition to material-specific scatter, can lead to a high testing-related scatter. The comparatively high testing effort involved in the test methods known from the literature [1-5] and the error-prone centric load application can lead to inaccurate and non-representative tensile strength values and hence to high standard deviations and a low reproducibility. Generally, the centric tensile strength tests are significantly influenced by the following parameters:

- 1) Material scatter (inhomogeneity, pre-damage due to preparation etc.);
- 2) Production of the test specimens (dimensional stability, homogeneity etc.);
- 3) Clamp (inaccuracies, eccentricity in load application, application to the testing machine etc.);
- 4) Handling (specimen installation etc.);
- 5) Testing machine (relative repeatability, display deviation, eccentricity etc.).

In addition to the setup mentioned in [3,4], bone-shaped specimens according to ASTM C307-18 [6] can be used to determine the centric tensile strength, cf. Figure 2a. In ASTM C307-18 [6], the specimens are pulled centrally using clamps as shown in Figure 2b. The experimental setup, especially the mounting shown in Figure 2b, hereafter referred to as C-Type, was used by [1,2,7]. The test method was verified in interlaboratory studies, which were carried out by six different facilities in 2017 [8]. The laboratories conducted 3 test series with 6 individual tests each on a chemical resistant grout with a tensile strength of about 14.6 MPa. The test method was validated by evaluation of repeatability and reproducibility [8]. For the tests the variation coefficient for repeatability and reproducibility is about 7%.

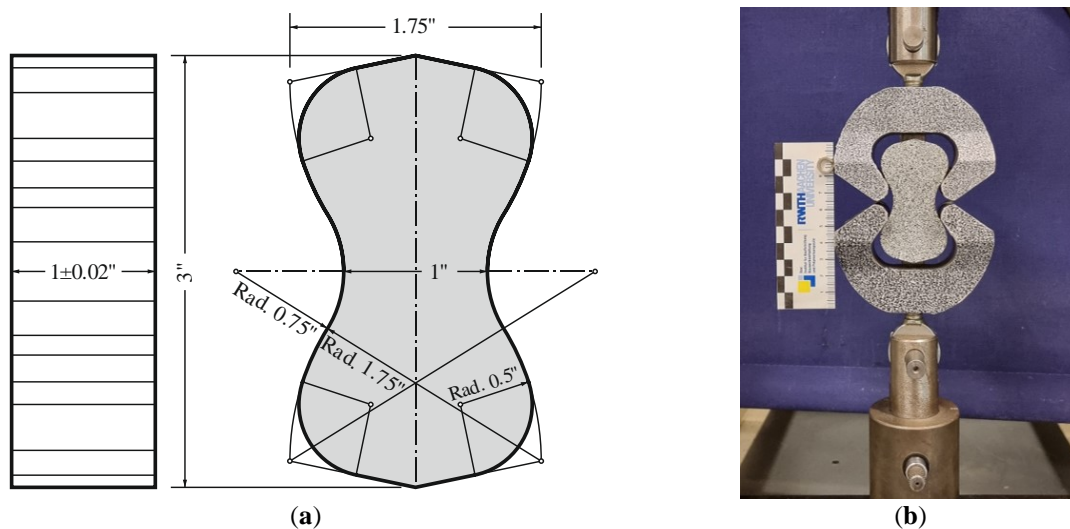


**Figure 2.** Tensile Strength Test Setup acc. to ASTM C307-18 [6]. (a) Briquet specimen (technical drawing); (b) C-Type clamps flexibly mounted on both sides in the testing machine with specimen.

According to ASTM C307-18 [6], a minimum of 6 briquet specimens for each material have to be tested at a crosshead speed of 5 to 6.4 mm/min and a temperature of  $23 \pm 2$  °C. The tensile strength  $S$  is calculated according to equation (1) as division of the load  $P$  at the moment of crack per surface area [6]:

$$S = P / (b \cdot d) \quad (1)$$

with:

$S$  = tensile strength;  $P$  = load at the moment of crack;

$b$  = width at the waist of the briquet tested;  $d$  = depth of briquet tested

The ASTM C307 has already been used and further developed for many fields of application. For example, [7,9] used the tensile strength tests with the experimental C-Type setup to determine the influence of sulfate attack on different binders as a function of varying storage conditions. The test setup was adapted by [10] for experiments at temperatures up to 200 °C to investigate the temperature dependent behavior of polymer adhesives. In another investigation, [11] used the test setup according to ASTM C307 analyzing the results with Weibull statistics to determine the tensile strength of a reference Class G cement slurry reinforced with inorganic micro-fibers. To investigate the influence of the specimen geometry, bone-shaped specimens, cylinders and a free form glued on steel stamps were investigated in [1]. In [1,4], the dimensions of the bone-shaped specimens as well as the clamps used for testing were upscaled by a factor of three. In addition, the outer form of the clamps was made rectangular. With the upscaled bone-shaped test specimens and the modified test setup tensile strength values with variation coefficients of maximum 10% were achieved [1]. In summary, various tests with the C-Type according to ASTM C307-18 [6] were conducted at the Institute of Building Materials Research, RWTH Aachen University, by [1,3-5,7,9].

In own preliminary tests on a repair mortar (RM-A4) for normal strength concrete with the C-Type according to ASTM C307-18 [6], a high standard deviation with a variation coefficient of 16.4% was observed. Deformations were recorded with the optical 3D-measurement system ARAMIS® from GOM GmbH. The displacement analysis was carried out with ARAMIS® Professional Software. The evaluation of the deformations indicated displacement and torsion of the samples in all three dimensions during the test. In principle, torsion of the specimen is acceptable, but should be completed above a certain load level before the maximum load is reached, so that the tensile stresses in the horizontal waist are uniformly directed perpendicular to the plane. If torsion continues until fracture occurs, an uneven stress distribution must be assumed. Figure 3 shows exemplarily the displacement of four measurement points on the specimen surface during tensile testing. The placement of the surface points was chosen analogous to Figure 4 (cf. chapter 2.2). The measurement points indicate an increase in displacement and differences between the points indicating a constant torsion of the specimen throughout the experimental test.

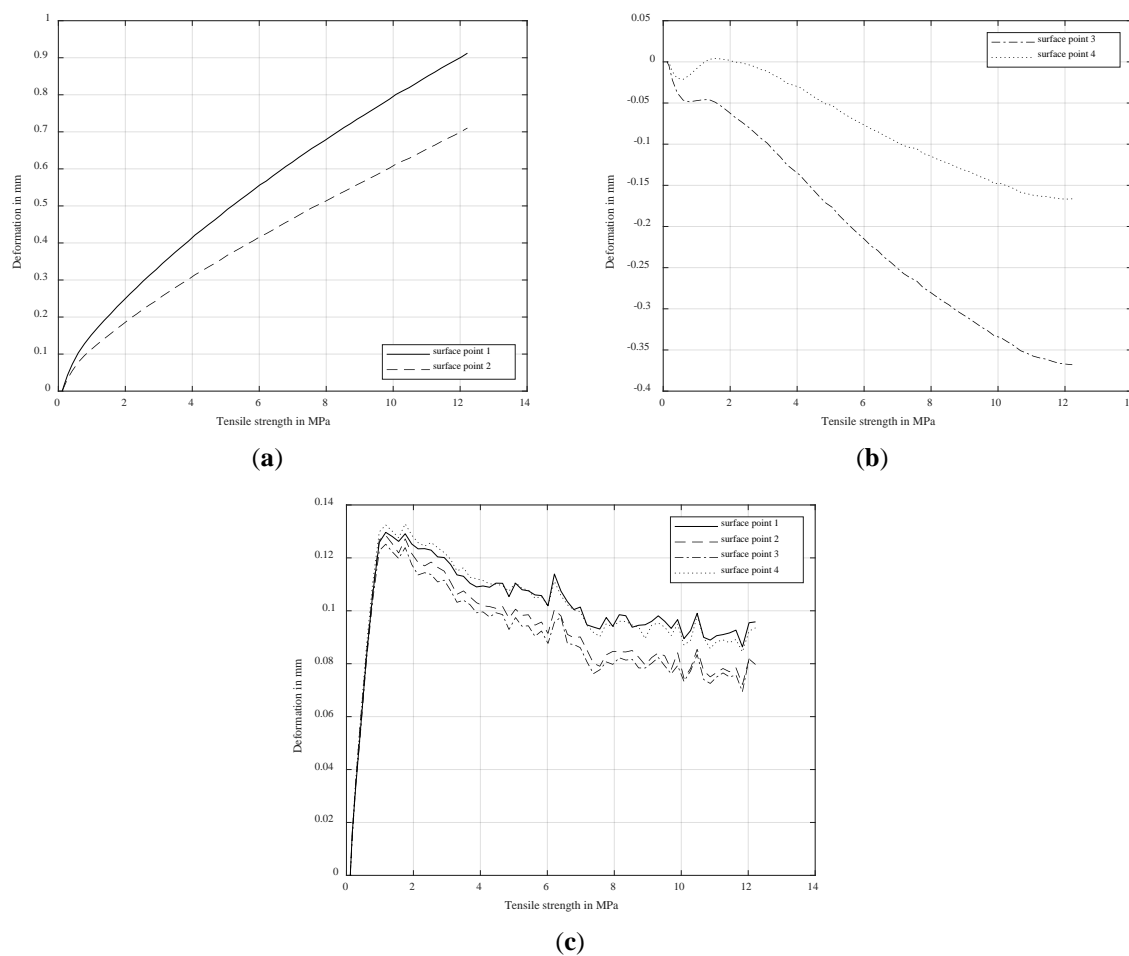


**Figure 3.** Deformation analysis on surface evaluation points: (a) x-axis displacement, (b) y-axis displacement, (c) z-axis displacement.

The preliminary tests indicated that a minimum change in position of 0.1 mm leads to a reduction of the deformation differences of about 39%. Therefore, efforts were taken to reduce the non-material specific deviations of the test results. Within the following investigations, for example, the positioning of the test specimens as well as the mounting of the clamps was varied. Based on the preliminary tests, the test setup according to ASTM C307-18 [6] was further developed to obtain reliable, reproducible test results with a lower standard deviation. In addition, the “Setup Testing Tool” was used in the optical 3D-measurement software to maintain the same initial testing position for each test. This tool allows to vary and adjust the position of the specimen manually via live measurements on the surface of a positioning adapter, which was developed for this purpose.

In the further developed experimental setup tensile strength tests were implemented according to ASTM C307-18 on three mineral-based materials with varying tensile strength properties in the range of 0.4 to 5.9 MPa, thus deriving values for the main test parameters such as test speed, preload and the recommended number of samples of a test series. The number of samples was determined to obtain representative results with the minimum possible number of samples.

## 2. Methods and materials

### 2.1 Experimental setup and preliminary tests

The further developed test setup as well as the applied materials are described below. In preliminary tests, the C-Type test setup according to ASTM C307-18 [6] was used for investigating the centric tensile strength on a repair mortar RM-A4 according to [6]. For the tests a universal testing machine Zwick ZMART.Pro with a 10 kN load cell and a relative repeatability (3 values) of 0.12% (tensile load 5000 N) to 0.50% (100 N) and a display deviation of -0.12% (1000 N) to 0.12% (200 N) was used. In the preliminary tests, the load was applied at a constant crosshead test speed of 5 mm/min.

To optimize the test setup, various tests were carried out with a steel bone-shaped specimen, milled from 42CrMo4 steel according to the geometry of Figure 2a. The steel specimen was loaded up to 8 kN and then unloaded again. The load and the crosshead displacement were recorded in the software TestXpert® and then transferred to the optical 3D-measurement system. Tests were carried out with the upper clamp alternately mounted rigidly and flexibly to analyze the deformation in the x- and y-axis.

Based on the findings of the preliminary tests, the geometry of the clamps in [6] were modified adapted from [1], further described as U-Type. The results shows that both the upper and lower clamps should be firmly mounted to the machine. Thus, lateral supports were implemented to prevent deformation in the x- and y-axis. The friction influence of the screws on the lateral supports was also investigated by varying the applied torque from 1 to 10 Nm.

Further, the installation of the test specimen was then optimized with the developed adapter for positioning, abbreviated as PA, and varying specimen positions. The selected position was verified in further experiments. Table 1 gives an overview of the test series during optimization of the experimental setup.

**Table 1.** Overview of the preliminary test series.

Test setup type	Investigated parameter	Material	Number of tests
C-Type	Reference tests	Mortar RM-A4 <sup>1)</sup>	6
	Fixed & flexible upper clamping	Steel	5
	Fixed lower & flexible upper clamping	Steel	15
U-Type	Fixed lower and upper lateral supports	Steel	17
	Investigation of the friction: Torque of the screws from 1 to 10 Nm (upper and lower fixing)	Steel	20
U-Type with PA	Varying Positions	Steel	22
	Final test setup & position	Steel	10

<sup>1)</sup> Batch 1, cf. Table 2, chapter 2.3

### 2.2 Experiment evaluation method

#### 2.2.1 Optical 3D deformation analysis

The evaluation of the experimental tests was carried out with the optical 3D-measurement system ARAMIS®. For this purpose, the evaluation methods are described hereinafter. For the optical deformation analysis, a stochastic pattern is applied on the formwork side of the specimen. First, a white primer is applied, then a black lacquer is sprayed creating the required contrast. Before starting the experiments, the optical 3D-measurement system was calibrated with the calibration plate CP20 90 x 72 mm. The measuring accuracy between two 19 x 19 pixel facets with an overlap of 3 pixels and 5M pixel cameras with an aperture of 5.6 mm is approximately

98,61%. In the calibration of the test, the measurement volume is determined, a reference image is created and thus the measuring surface of the test is defined. After the tests, the x-axis and y-axis of the existing alignment was offset to the center of the specimen by means of the 3-2-1 transformation option. The origin of the z-axis was set on the measuring surface. This coordinate system was defined in all experiments at the same position further known as nominal coordinate system, cf. Figure 4.

For the deformation analysis, 5 images per second were taken. The image upon reaching the preload was selected as the reference stage. For evaluation, a surface component was defined on the measuring surface of each specimen with a stochastic pattern. Further, four surface points were set to compare the displacement and torsion of each test specimen. These points were each placed at a distance of 9 mm from the origin of the nominal coordinate system and the difference of the displacements in the points was calculated at 1/3 of the maximum tensile force. For the x-axis, points 1 and 2 were used for the displacement on the x-axis, points 3 and 4 were used for the displacement on the y-axis. The difference between the minimum and maximum displacement of points 1-4 were used to calculate the displacement on the z-axis (cf, Figure 4).

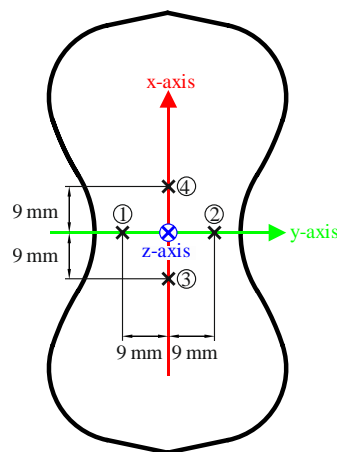


**Figure 4.** Nominal coordinate system and position of the surface points for optical 3D-deformation analysis.

### 2.2.2 Positioning adapter

The aim was to place all specimens in the same initial position by means of an adapter, thus to reduce the testing differences. For this purpose, a positioning adapter (PA) was developed and 3D printed, cf. Figure 5a. To position the bone-shaped specimens, the PA was placed on the specimen surface, cf. Figure 5b. The depth and surface shape of the PA were adjusted to allow the adapter to be removed without changing the specimen position. A total of 8 point markers were adhered to the adapter enabling a live measurement in the optical 3D-measurement software. Using the live measurement, the displacement of the specimen position can be visualized, cf. Figure 5b. For this purpose, an opto-mechanical self-defined adapter was created in the optical 3D-measurement software [12]. The coordinate system of the adapter was defined based on the 8 point markers. A local coordinate system was defined for the upper and fixed lower clamps based on point markers on the clamps.

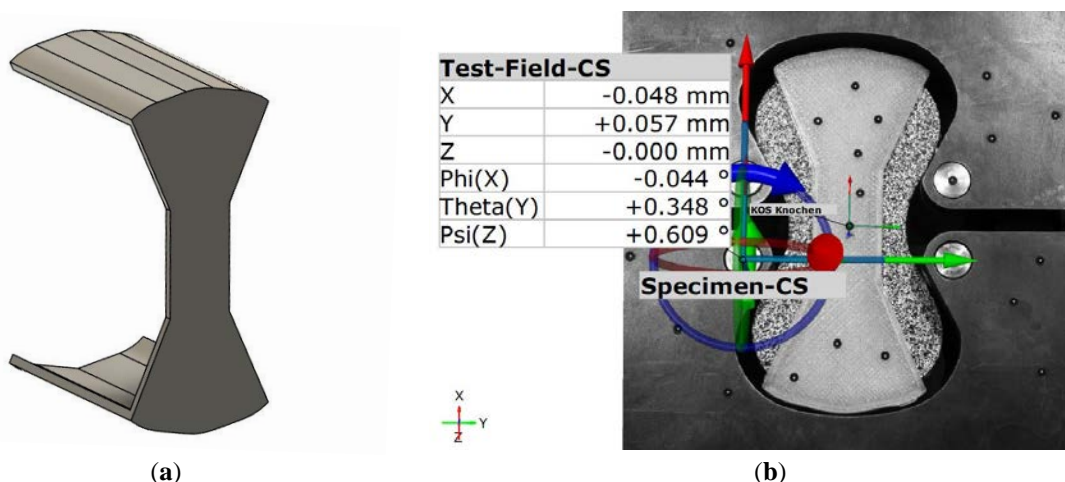


**Figure 5.** Positioning Adapter (PA): (a) 3D schematic drawing of the PA; (b) Specimen and PA in the test setup with exemplary deviation values of the specimen's position in relation to the nominal coordinate system.

To find out the optimum position of the test specimen, the position of the steel bone-shaped specimen was varied in initial tests. Therefore, the specimen with the adapter was positioned between the clamps. The specimen position is displayed live in the software, cf. Figure 5b, and can be manually adjusted to the desired test position. The specimen was tested according to 2.1. The displacements of the specimen were evaluated as described in 2.2. The test with the smallest deviations was chosen as the optimum position, cf. Table 2. In additional tests, the selected position was verified. The selected position was then chosen as the offset in the tests with the mineral-based materials.

Before testing the positioning was carried out for the x-, y- and z- axis. A maximum deviation of  $\pm 0.1$  mm and torsion of  $\pm 1^\circ$  was defined.

### 2.3 Applied materials

Tensile strength tests of mineral-based materials in the range of 0.4 to 5.9 MPa were implemented according to ASTM C307-18 in the U-Type test setup. The following three building and repair materials with varying mechanical properties were selected for the experimental investigations, covering the lower to middle range of the 10 kN load cell of the testing machine:

- 1) Repair Mortar (RM-A4);
- 2) Pointing Mortar developed for Aachen Cathedral (PM21);
- 3) Autoclaved Aerated Concrete (AAC2-350).

Bone-shaped briquet specimens of the three materials are shown in Figure 6.



**Figure 6.** Bone-shaped briquet specimens of the three materials (exemplarily): (1) RM-A4, (2) PM21, (3) ACC2-350

#### 2.3.1 Repair mortar RM-A4

The commercially available repair mortar RM-A4 according to [13,14] is a polymer-modified cement-based mortar designed for repairing or retrofitting horizontal, vertical and overhead concrete surfaces. Due to the compressive strength of about 66 MPa at the age of 27 days, the mortar was selected in order to test the middle load range of the testing machine.

RM-A4 was mixed according to the manufacturer's specifications in a ratio of solid to water weight content of 1:0.13. Subsequently, the fresh mortar properties were determined for each batch according to [15] (consistence), [16] (bulk density) and [17] (air content). Standard prism sets (each prism with 160 mm in length and 40 mm in width and height [18]) to determine the flexural and compressive strength for the respective test date of the tensile tests were prepared in accordance with [19]. The repair mortar was poured into briquet molds and compacted with a vibrating table. The test specimens were stripped of the formwork after one day and stored in humid climate for 7 days. Afterwards, the specimens were stored in a climate room at a temperature of  $20 \pm 1$  °C and a relative humidity of  $53 \pm 8\%$  until testing at the age of 27 and 103 days, respectively. The fresh and solid mortar properties are given in Table 2.

#### 2.3.2 Pointing mortar PM21

The PM21 pointing mortar is adapted to the properties of the historic natural stone masonry of the choir hall of Aachen Cathedral. The binder system consisting of White Portland cement and composite cement with natural pozzolan, calcium hydroxide and silica fume is combined with Quartz flour, sand and gravel with a maximum grain size of 4 mm. The mortar contains various lightweight aggregates to achieve a load-bearing and deformation behavior adapted to the natural stone masonry. In addition, a small amount ( $< 1$  wt.%) of additives and admixtures are added to the mortar to adjust essential fresh and solid mortar properties such as workability or bond properties.

Based on the compressive strength, the mortar can be assigned to strength class M5 according to [20] with a compressive strength of about 7.1 MPa, a flexural strength of about 3.2 MPa and a modulus of elasticity of about

4.3 GPa, each at the age of 28 days. The corresponding dry bulk density is about 1300 kg/m<sup>3</sup>. Compared to the RM-A4, the compressive strength of PM21 is about 11.5% of RM-A4. The expected maximum load was less than 500 N, which is about 5% of the maximum load of the load cell of the testing machine.

Two batches of PM21 were mixed in a ratio of solid to water weight content of about 1:0.30. Subsequently, fresh mortar properties were determined in accordance with [15-17]. Standard prism sets to determine the flexural and compressive strength for each respective testing time of the tensile tests were prepared in accordance with [19]. Finally, the mortar was poured into briquet molds and compacted with a vibrating table. The test specimens were stripped of the formwork after two days and stored in humid climate for 7 days of age. Afterwards, the specimens were stored in a climate room at a temperature of  $20 \pm 1$  °C and a relative humidity of  $53 \pm 8\%$  until testing at the age of 27 and 28 days, respectively. The fresh and solid mortar properties are given in Table 2.

### 2.3.3 Autoclaved aerated concrete AAC2-350

In order to set up the test matrix broadly regarding the mechanical properties, Autoclaved Aerated Concrete with low strength representing the lower accuracy range of the 10 kN load cell was investigated, too.

The applied AAC2-350 can be assigned to strength class 2 according to [21] with a compressive strength of about 2.9 MPa, tested according to [22] on cubes with an edge length of 100 mm. The dry bulk density of about 310 kg/m<sup>3</sup>, also tested on 100 mm cubes, according to [23], corresponds to the density class 0.35 according to [24]. Compared to the RM-A4, the compressive strength of AAC2-350 is about 4.5% of RM-A4. The expected maximum load was less than 200 N, which is about 2% of the maximum load of the load cell of the testing machine.

For the tests, each 6 samples were taken from the middle third of 6 different AAC units. To prepare the specimens, discs with a length of about 200 mm, a width of about 100 mm and a height of about 30 mm were cut out of the units by dry cut. To prevent effects of carbonation the discs were preconditioned in argon atmosphere to a moisture content less than about 20 wt.% which allowed the discs to be ground to a thickness of about  $25.4 \pm 0.4$  mm and milled with a CNC mill. Finally, the briquets were conditioned again to a moisture content of about  $6 \pm 2$  wt.% in argon atmosphere and preserved in vacuum bags until testing.

### 2.3.4 Mortar properties

In addition to the material properties described for RM-A4 and PM21, the determined fresh and solid mortar properties with indication of the testing age is summarized in Table 2.

**Table 2.** Fresh and solid properties of the applied mortars.

Mortar	Batch	Fresh mortar			Solid mortar		Age
		Consistence	Bulk density	Air content	Flexural strength	Compressive strength	
		mm	kg/m <sup>3</sup>	vol. %		MPa	d
RM-A4	1	142	2180	4.5	10.4	78.5	103
	2	141	2170	4.4	10.5	63.9	27
	3	140	2190	4.2	11.4	67.8	27
PM21	1	114	1530	13.0	3.4	7.7	28
	2	124	1490	14.0	2.9	6.5	27

### 2.3.5 Experimental test program

For each of the applied materials, first the preload and the crosshead-controlled test speed were varied to find out the optimum parameters for testing the tensile strength. Maximum 10% of the expected tensile load was aspired as the maximum preload. Afterwards 15 and 18 tests, respectively, with defined test parameters were conducted to determine the representative number of samples of a test series. The tests were performed at a room temperature of  $18.5 \pm 2$  °C. Table 3 shows the established parameters of the test series.

For the tensile tests, the U-Type test setup was used and the bone-shaped specimens were installed in the defined position using the PA and the tool in the optical 3D-measurement software, as described in chapter 2.2. To evaluate the tensile tests, the deformations of the specimens in x-, y- and z-axis were recorded by means of optical 3D-measurement, too. Therefore, the specimens were prepared with the stochastic pattern. After testing, the deformations of defined surface points were evaluated at a load of 1/3 of the tensile strength and compared to the deformations at the initial state, when load application started. The test results were evaluated regarding the calculated mean values and standard deviations of the deformation differences in x-, y- and z-axis. Afterwards, the recommended preload and test speed were defined.

To derive the required number of samples of the applied materials, the test results were statistically analyzed. First it was verified, if the tensile strength values for each test series follow the normal distribution. For this purpose, the parametric tests according to Kolmogorov-Smirnov and Shapiro-Wilk, as given for example in [25], were applied. As a result, the normal distribution is given for all tensile strength values of each test series. The

anticipated values of the tensile strength were determined for each test series. For a 95% confidence interval, the required number of samples  $n$  of a test series was calculated according to [26] using equation (2) with the total number of samples  $N$ , the constant factor  $z = 1,96$  given in [26] for standard normal distribution and the standard deviation  $s$ .

$$n = \frac{N \cdot (1,96 \cdot s)^2}{(1,96 \cdot s)^2 + (N - 1) \cdot (0,05 \cdot x_{mean})^2} \quad (2)$$

With:

$n$  = required number of samples

$N$  = total number of samples

$s$  = standard deviation

$x_{mean}$  = mean value of the tensile strength

**Table 3.** Defined test parameters of the tensile tests on the three applied materials.

Material	Test series	Test parameter		Number of tests
		Preload [N]	Test speed [mm/min]	
RM-A4	Preload	0	5	9
		100		
		200		
	Test speed	200	0.1 0.6 2	9
	Number of samples	200	0.6	18
PM21	Preload	40	0.6	9
		80		
		100		
	Test speed	80	0.3 1 2	9
	Number of samples	80	0.6	15
AAC2-350	Preload	0	0.4	9
		15		
		25		
	Test speed	25	0.7 1 3	9
	Number of samples	25	0.6	18

### 3. Results

#### 3.1 Improved experimental Setup

In the preliminary tests with RM-A4 and a preload varying between 0 to 100 N, a mean tensile strength of 5.2 MPa with a standard deviation of 0.86 MPa and a variation coefficient of 16.4% could be determined for this test series. The further tests were carried out with the steel bone-shaped specimen. It was determined that by adjusting the clamping in the y-direction as described in chapter 2.1, an average displacement of 0.13 mm was obtained with ARAMIS®. In z-direction, an average tilting movement of 0.07 mm with maximum values of 0.24 mm were determined.

To further develop the test setup, the C-Type test setup was varied on the basis of [1,6]. Adapted from [1], a rectangular outer clamp geometry was chosen, cf. Figure 7a. The inner dimensions were not adjusted and comply with ASTM C307-18 [6]. This new clamp was produced of 42CrMo4 steel in a CNC milling machine. In addition, lateral supports were added via 42CrMo4 steel rails, cf. Figure 7b, which can either be attached to the upper or the lower clamp. The aim was that the lateral supports would prevent the clamps from being displaced in the y- and z-direction and allow a centric pull in x-direction. The developed experimental setup is shown in Figure 8. The U-Type compared to the C-Type is laterally fixed by steel supports and the mounting of the lower clamp cannot be installed flexibly.

With the U-Type, the tests were repeated on the steel specimen, starting by screwing the lateral supports to the lower clamp by hand. Both clamps were firmly fixed at the top and bottom. As can be seen in Table 4, this already leads to less deformation of the specimen during the test. The tensile loading was repeated several times and



subsequently the lateral supports were screwed at the top upper clamp in a further series. When comparing the upper and lower installation of the lateral supports, the lower installation can minimize the deformation of the specimen.

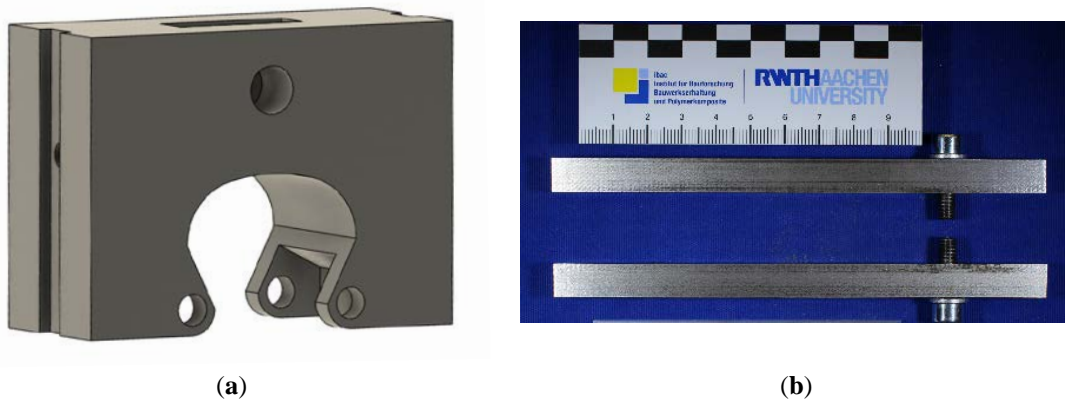


**Figure 7.** U-Type: (a) 3D schematic drawing of the upper clamp; (b) Lateral supports.

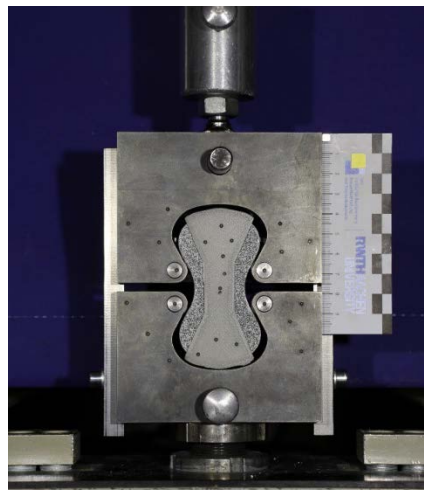


**Figure 8.** Developed experimental setup.

**Table 4.** Deformations at a tensile stress of 6 MPa.

Type	Description	Value [mm]	$\Delta x$		$\Delta y$		$\Delta z$	
			MV	SD	MV	SD	MV	SD
C-Type	Base equipment	Value [mm]	0.127	0.074	0.131	0.069	0.071	0.083
	Lateral supports bottom fixed	Value [mm]	0.009	0.007	0.009	0.007	0.029	0.013
U-Type	Lateral supports top fixed	Value [mm]	0.023	0.016	0.023	0.016	0.020	0.008
	Flexible upper clamp	Value [mm]	0.044	0.042	0.044	0.042	0.020	0.015
	Final test setup	Value [mm]	0.009	0.008	0.009	0.007	0.022	0.007
	Improvement [%] <sup>1)</sup>		92.9	91.7	85.7	92.5	94.5	95.3

MV = Mean Value; SD = Standard deviation

<sup>1)</sup> Percentage reduction of the deformation differences in relation to the C-Type.

Further tests were carried out with a flexible upper clamp. However, this leads to larger deformations differences in x- and y-direction compared to the tests with fixed clamping. Based on the deformations of the specimen, it was established that the tensile strength tests can be performed uniaxial with a low standard deviation if the clamps are

fixed and the lateral supports are attached to the lower clamp. To verify this, a number of tests were carried out and evaluated. The difference between the mean value and the standard deviation is smaller for the final U-Type, and the overall deformation of the specimen is significantly reduced.

To visualize the displacement differences between the C- & U-Type test setups, the deformation evaluation obtained with digital image correlation ARAMIS® of the steel sample is shown in Figure 9.

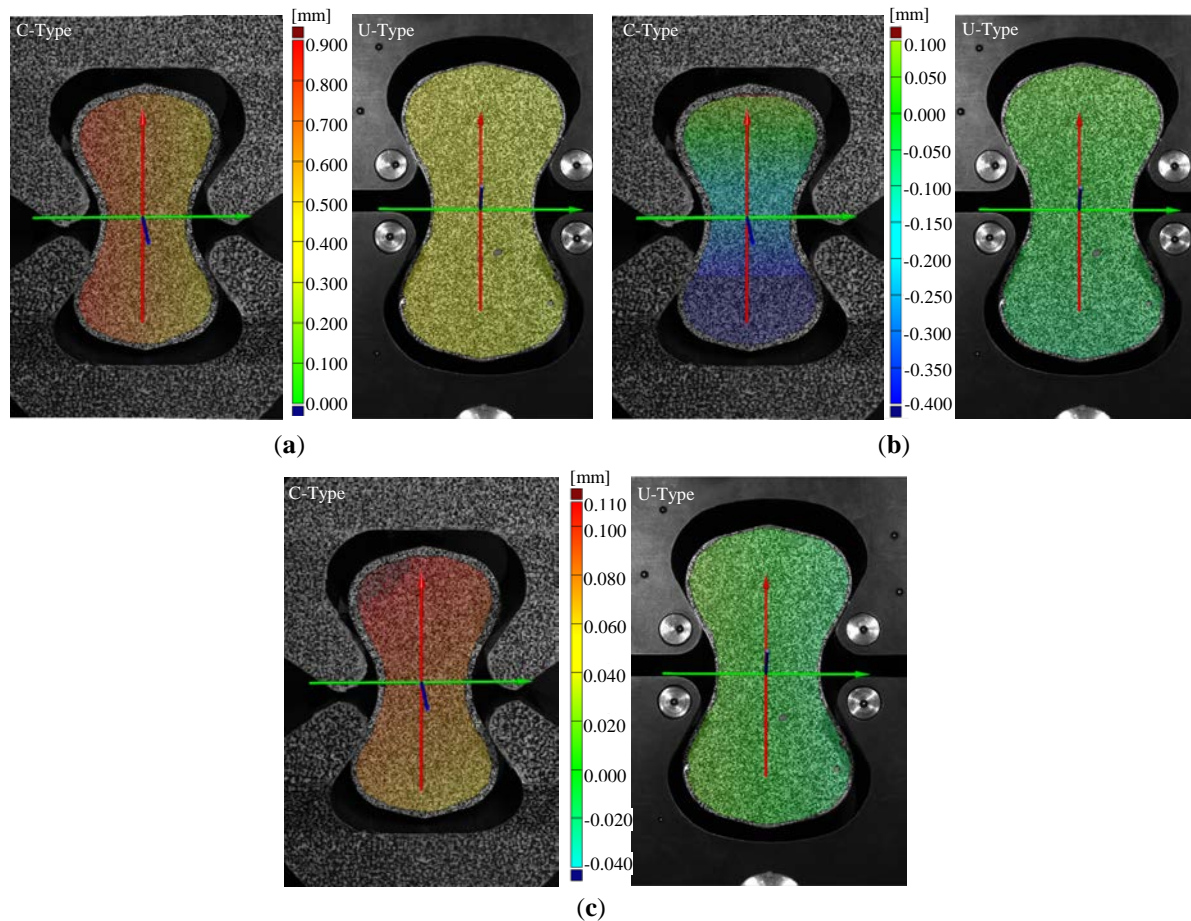


**Figure 9.** Optical 3D deformation analysis for C- & U-Type test setup at 6 kN: (a) x-axis displacement, (b) y-axis displacement, (c) z-axis displacement.

To determine the frictional influence of the lateral supports, tensile tests without test specimens were conducted with different degrees of the torque wrench for tightening the lateral supports. Figure 10 shows the frictional force as a function of torque. It can be seen that the friction is not significantly increased by tightening the fasteners. Based on this result, it was specified that the screws are tightened manually, which corresponds to a torque of 7 to 8 Nm.

With the U-Type setup, the optimal position of the specimen for the test was investigated. For this purpose, the PA presented in chapter 2.1 was used and the position of the bone-shaped steel specimen was varied. The position change in relation to the nominal coordinate system was examined via the exports in the Setup Testing Tool and the effect of the position change was evaluated via the deformation of the set points in ARAMIS®.

In experiments, the bone-shaped test specimen was installed in the test facility offset in the z-axis. In addition, the height of the upper clamp was varied. Based on the displacement evaluation, a position was selected and applied as x-, y- & z-offset in the Setup Testing Tool. In each case, this offset refers to the lower clamp as the reference point. Subsequently, the position was varied, since the combination of the coordinates of the x-position clamp and x-position specimen had to be adjusted in relation to the lower clamp. The selected position was verified in 10 tests and low standard deviations were achieved in the tensile strength. The following Table 5 exemplarily shows the results of selected experiments.

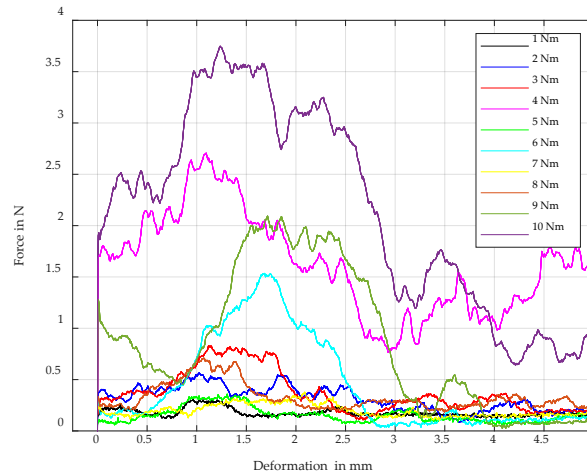


Figure 10. Frictional force as a function of torque.

Table 5. Deformations differences for different test configurations.

Description		Position Clamp			Position Specimen			Deformation Differences		
		x	y	z	x	y	z	$\Delta x$	$\Delta y$	$\Delta z$
Specimen further forward	Value [mm]	17.29	1.17	-0.63	8.50	22.53	7.26	0.023	0.022	0.027
Specimen further back	Value [mm]	17.31	1.10	-0.49	8.58	22.46	4.89	0.026	0.025	0.012
Upper clamp higher	Value [mm]	17.51	1.05	-0.45	8.58	22.19	5.58	0.020	0.019	0.010
Set position of a test series [mm]	Mean value	17.45	1.05	-0.44	8.53	22.25	5.17	0.013	0.013	0.006
Final position of a test series [mm]	Mean value	17.45	1.05	-0.44	8.60	22.41	5.17	0.014	0.014	0.018

### 3.2 Tensile tests

With the three different materials, tensile tests were carried out in the new U-Type test setup and evaluated in the optical 3D-measurement software. A recommendation was made for similar materials in terms of test speed, preload and the statistically required number of specimens in a test series.

#### 3.2.1 Repair mortar RM-A4

For the repair mortar, the most constant results for the test series with different preloads at a constant test speed of 5 mm/min [6] were obtained for a preload of 200 N. The results of the test series with different preloads are shown in the Table 6.

In the investigation of the preload, the largest deformation with a preload of 0 N was observed in the crosshead movement. This can be explained because a preload greater than 0 N leads to setting of the specimens. In the evaluation of the specimen deformation, only a low deviation can be seen in the x and y directions. The lowest torsion of the specimen was observed at a preload of 200 N for the z-axis, see Table 5. Based on the results of the deformation, a preload of 200 N was selected for the tests with varying test speeds. The variation of the test speed shows an increase of the tensile strength the higher the test speed is. The lower the test speed, the lower the standard deviation of the tensile stress. Further, at a test speed of 0.1 mm/min, the deformation of the specimens is highest and a creep behavior is induced in the mortar due to the low speed. To prevent this, the aspired test time was set to approx. 1 min, as suggested in [19]. This results in the selection of a test speed of 0.6 mm/min based on the results of the crosshead displacement.

For the repair mortar, the normal distribution with an expected value of 5.89 MPa at the density of 1.25 as shown in Figure 11 is obtained. Equation (2) results in a number of 4 specimens per test series.

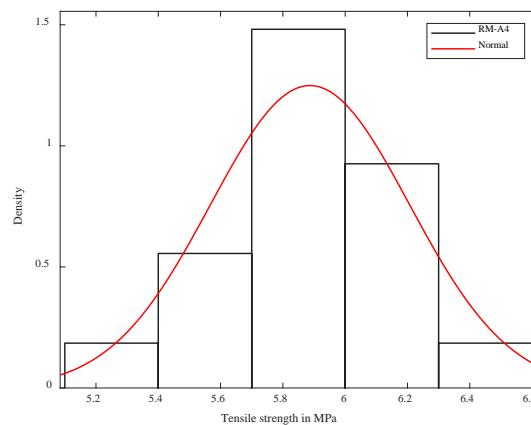
For the RM-A4, a ratio between tensile and compressive strength of 9% was determined. The ratio was calculated by determining the compressive strength on standard prisms according to [18] and the average value of the tensile tests.

**Table 6.** Results of the test series RM-A4 with specification of the preload, test speed and number of samples.

Series	Batch	Varied parameters	Number of tests	Tensile strength		Crosshead displacement		Deformation differences					
				MV	SD	MV	SD	$\Delta x$		$\Delta y$		$\Delta z$	
				[MPa]	[MPa]	[mm]	[mm]	MV	SD	MV	SD	MV	SD
Preload <sup>1)</sup>	2	0 N	3	5.47	0.45	0.79	0.10	0.007	0.008	0.008	0.009	0.041	0.004
		100 N	3	6.15	0.17	0.68	0.02	0.008	0.006	0.007	0.007	0.008	0.004
		200 N	3	5.91	0.23	0.61	0.02	0.007	0.003	0.008	0.002	0.005	0.003
Test Speed <sup>2)</sup>	2	0.1 mm/min	3	5.14	0.15	0.55	0.01	0.011	0.000	0.010	0.000	0.002	0.002
		0.6 mm/min	3	5.45	0.13	0.58	0.03	0.003	0.001	0.003	0.001	0.008	0.011
		2 mm/min	3	5.41	0.24	0.59	0.02	0.004	0.003	0.005	0.002	0.021	0.009
Final parameters, investigation sample number	3	200 N, 0.6 mm/min	18	5.89	0.32	0.63	0.03	-	-	-	-	-	-

MV = Mean value; SD = Standard deviation

<sup>1)</sup> Series with test speed 5 mm/min; <sup>2)</sup> Series with preload 200 N

**Figure 11.** Normal distribution repair mortar RM-A4.

### 3.2.2 Pointing mortar PM21

Regardless the applied preload, mean tensile strength values of 1.47 to 1.49 MPa were achieved in the first series with a constant test speed of 0.6 mm/min, cf. Table 7. The maximum crosshead displacement recorded during the tensile tests decreases slightly with increasing preload. The lowest differences in deformation of the specimen were recorded at a preload level of 80 N, which is why this preload level was defined for the test speed series, cf. Table 7.

A very slow test speed, which was selected for the RM-A4 and which usually leads to creep effects during the tensile test, was not used for the PM21. Instead, the test speed was varied between 0.3 and 1 mm/min. The tensile strength values achieved with those test speeds are identical at 1.47 and 1.48 MPa. The recorded maximum mean crosshead displacement is also the same at 0.53 mm. A test speed of 2 mm/min chosen as the upper test speed limit resulted in a higher maximum tensile strength of 1.54 MPa with a lower maximum crosshead displacement of 0.50 mm, cf. RM-A4.

The trend observed for RM-A4 that a lower test speed is accompanied by a lower standard deviation could not be confirmed for PM21.

For PM21, the deformation doesn't seem to be a reliable criterion for choosing a suitable test speed, since, the calculated deformation values for the selected test speeds of 0.3 mm/min and 2 mm/min are nearly the same. More important for the performance of the tensile test was a suitable test duration, cf. RM-A4. For this purpose, the test duration for testing the PM21 was also set to approx. 1 min. Regarding the observed crosshead displacement the test speed for the test series "number of samples" first was set to 0.55 mm/min.

First, three tests were performed with a preload of 80 N and a test speed of 0.55 mm/min. Since the specimens taken for this test series were of lower strength compared to those tested in the first two series, accompanied with higher deformations, the test parameters were adjusted to 80 N and 0.6 mm/min. The mean tensile strength of this test series was 1.40 MPa with a standard deviation of 0.14 MPa and a variation coefficient of 9.6%. At a 5% significance level ( $\alpha = 0.05$ ), equation (2) yields a recommended number of samples of 8.

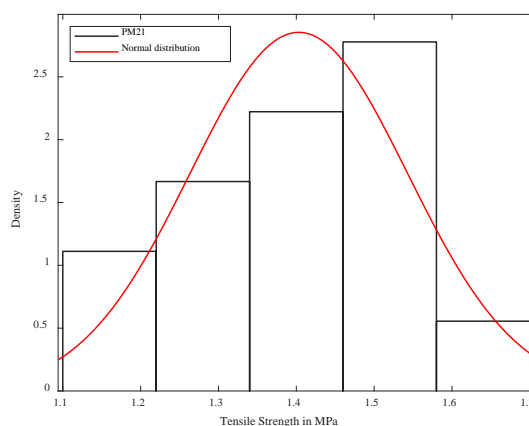
**Table 7.** Results of the test series PM21 with specification of the preload, test speed and number of samples.

Series	Batch	Varied parameters	Number of tests	Tensile strength		Crosshead displacement		Deformation differences					
				MV	SD	MV	SD	$\Delta x$		$\Delta y$		$\Delta z$	
				[MPa]	[MPa]	[mm]	[mm]	MV	SD	MV	SD	MV	SD
Preload <sup>1)</sup>	1	40 N	3	1.49	0.10	0.57	0.05	0.003	0.002	0.003	0.002	0.010	0.003
		80 N	3	1.48	0.07	0.55	0.05	0.003	0.001	0.003	0.001	0.006	0.004
		100 N	3	1.47	0.13	0.48	0.08	0.005	0.002	0.004	0.002	0.009	0.004
Test Speed <sup>2)</sup>	1	0.3 mm/min	3	1.47	0.03	0.53	0.03	0.005	0.003	0.005	0.003	0.005	0.002
		1 mm/min	3	1.48	0.07	0.53	0.10	0.007	0.001	0.007	0.001	0.010	0.001
		2 mm/min	3	1.54	0.02	0.50	0.02	0.004	0.003	0.005	0.002	0.006	0.003
Final parameters, investigation sample number	2	80 N, 0.6 mm/min	15	1.40	0.14	0.66	0.13	-	-	-	-	-	-

MV = Mean value; SD = Standard deviation

<sup>1)</sup> Series with test speed 0.6 mm/min; <sup>2)</sup> Series with preload 80 N

For the PM21, the normal distribution with an expected value of 1.40 MPa at the density of 2.85 as shown in Figure 12 is obtained.

**Figure 12.** Normal distribution pointing mortar PM21.

### 3.2.3 Autoclaved aerated concrete AAC2-350

Overall, the tensile strength of AAC2-350 ranges from 0.37 to 0.43 MPa with a standard deviation of 0.00 to 0.04 MPa, see Table 8.

For determining the optimum preload, the preload was varied between 0 to 25 N, which corresponds to about 9% of the tensile strength obtained. As expected, performing the test without any preload led to the largest crosshead displacement, but on the contrary, also to the highest tensile strength and the lowest standard deviation of all preload levels. The preload of 15 N led to a very small mean value and standard deviation of the obtained deformation differences, which means, that there was nearly no torsion of the specimen to be observed during these tests. The third preload level with 25 N showed a constant initial gradient of all three load-displacement curves, why this load was chosen for the test speed series, although the twist of the specimens was higher compared to the preload level of 15 N.

The test speed was varied between 0.7 and 3 mm/min. The smallest deformation differences in x- and y-direction were obtained for a test speed of 0.7 mm/min, while the specimens tilted in z-direction, cf. Table 8. The smallest deformation differences in z-direction were obtained for a test speed of 3 mm/min. But, as previously described for RM-A4 and PM21, the test duration seems to be a more reliable criterion for choosing a suitable test speed than the deformation differences obtained. The test duration for testing the AAC2-350 should at least be set to 1 min. Based on the crosshead displacements a test speed of 0.6 mm/min was chosen to examine the number of samples required for the AAC2-350.

The test parameters were adjusted to 25 N and 0.6 mm/min. The mean tensile strength of this test series was 0.43 MPa with a standard deviation of 0.04 MPa and a variation coefficient of 8.9%. According to equation (2), a recommended number of samples of 8 can be set.

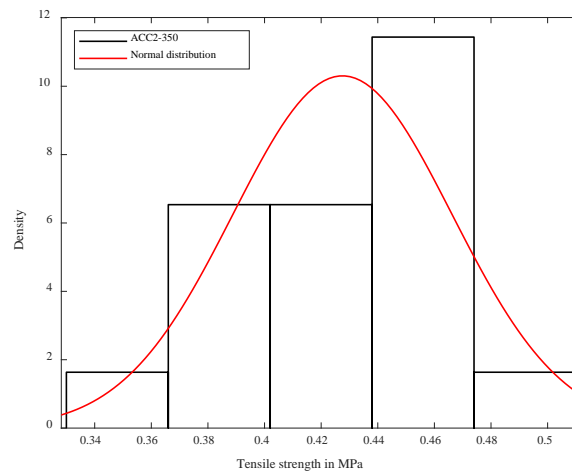
**Table 8.** Results of the test series AAC2-350 with specification of the preload, test speed and number of samples.

Series	Varied parameters	Number of tests	Tensile strength		Crosshead displacement		Deformation differences					
			MV	SD	MV	SD	$\Delta x$		$\Delta y$		$\Delta z$	
			[MPa]	[MPa]	[mm]	[mm]	MV	SD	MV	SD	MV	SD
Preload <sup>1)</sup>	0 N	3	0.42	0.01	0.90	0.03	0.159	0.244	0.026	0.020	0.063	0.027
	15 N	3	0.39	0.04	0.43	0.18	0.000	0.001	0.000	0.001	0.004	0.002
	25 N	3	0.39	0.04	0.72	0.15	0.009	0.004	0.009	0.003	0.016	0.011
Test Speed <sup>2)</sup>	0.7 mm/min	3	0.40	0.01	0.66	0.07	0.005	0.005	0.004	0.003	0.035	0.015
	1 mm/min	2	0.41	0.03 <sup>3)</sup>	0.69	0.10 <sup>3)</sup>	0.007	0.006 <sup>3)</sup>	0.008	0.006 <sup>3)</sup>	0.034	0.024 <sup>3)</sup>
	3 mm/min	3	0.37	0.00	0.62	0.06	0.007	0.003	0.008	0.003	0.017	0.006
Final parameters, investigation sample number	25 N, 0.6 mm/min	18	0.43	0.04	0.68	0.15	-	-	-	-	-	-

MV = Mean value; SD = Standard deviation

<sup>1)</sup> Series with test speed 0.4 mm/min; <sup>2)</sup> Series with preload 25 N; <sup>3)</sup> Standard deviation for 2 samples

For the AAC2-350, the normal distribution with an expected value of 0.43 MPa at the density of 10.3 as shown in Figure 13 is obtained.

**Figure 13.** Normal distribution AAC2-350.

### 3.2.4 Comparison

The tensile tests on RM-A4, PM21 and AAC2-350 were carried out with the improved experimental setup with the positioning tool. As reference values summarized in Table 9, an optimized preload, test speed and number of samples could be determined for the tested materials. The preload was determined depending on the tensile strength. The lower the strength, the lower the preload. The test speed is identical for all materials. In comparison, it can be observed that the crosshead displacement of the materials is the same despite their different tensile strength values. The selection of the test speed was made based on the test time as well as the crosshead displacement. The number of specimens was selected lowest for the RM-A4.

For the materials, the tensile strengths could be determined with a low standard deviation and variation coefficient. The highest coefficient of variation in comparison is shown by the test series of PM21. This can be attributed to the different grain structure present in the mortar. The distribution of the aggregate is different for each test specimen and can influence the tensile strength.

In the test series, the differences in the tensile strength values can be related to the different batches and the different testing times (for example 28 and 103 days). In comparison with the compressive strength, a ratio of 9% can be determined for the RM-A4, while the ACC2-350 has a ratio of 15% and the PM21 a ratio of 21%. The results should be considered with the influence of friction due to lateral supports.

**Table 9.** Comparison of the tensile and compressive strength.

Material	Preload $\beta_P$	Test speed	Number of samples	Crosshead displacement	Tensile strength $\beta_Z$			Compressive strength $\beta_D$		
					MV	SD	VC	MV	MV	$\beta_Z/\beta_D^{(2)}$
RM-A4	0.31	0.6	4	0.63	5.89	0.32	5.4	5.3	67.8	9
PM21	0.12	0.6	8	0.66	1.40	0.14	9.6	8.5	6.5	21
ACC2-350	0.04	0.6	8	0.68	0.43	0.04	8.9	9.3	2.9	15

MV = Mean value; SD = Standard deviation; VC = Variation coefficient

<sup>1)</sup>  $\beta_P/\beta_Z$  = Ratio of preload and tensile strength; <sup>2)</sup>  $\beta_Z/\beta_D$  = Ratio of tensile and compressive strength

#### 4. Conclusion and outlook

Within the framework of the investigations, factors influencing the centricity of the tensile tests, such as the specimen position at installation or the flexible mounting of the test setup and deviations in the lateral displacements of the clamps, were identified and quantified by digital image correlation in an optical 3D-measurement software. Based on the preliminary findings, the C-Type according to ASTM C307-18 [6] was further developed to U-Type. The clamps were firmly fixed at the bottom and flexible mounted at the top. The geometry of the clamps was modified according to [1] and enhanced with lateral supports fixing the clamps in the axial direction. To maintain the same starting position of each specimen, an adapter for specimens according to ASTM C307-18 [6] was developed and configured. The adapter tool and the bone-shaped steel specimen were used to find the optimal position in the new test setup.

The key findings of this work can be summarized as follows:

1) Overall, the improvements of the U-Type test setup in combination with the optimum positioning of the specimens led to a reduction in deformation differences and corresponding standard deviations of up to 94.5 and 95.3%, respectively, leading to a more uniform stress distribution in the cross section.

2) Regardless of the material strength, the crosshead test speed of 0.6 mm/min is adequate to obtain reasonable testing times of about 1 min.

3) With the further developed U-Type test setup, mineral-based materials with tensile strength values between 0.4 and 5.9 MPa can be tested in a reproducible manner with a variation coefficient smaller than 10%.

4) The laboratories by ASTM C307 conducted 3 test series with 6 individual tests each. In comparison, this study obtained that with a variation coefficient of about 5% the number of samples can be reduced to 4 specimens per test series. For a variation coefficient of up to 10% a number of 8 specimens for mineral-based materials should be tested.

5) The tensile to compressive strength ratio of about 10% as reported in the literature could not be verified for materials with low tensile strength with a ratio up to 21%, respectively, while the RM-A4 mortar confirmed the expected value with 9%.

In future studies, the testing equipment will be used to examine the influence of different environmental conditions as well as different temperatures during the test on the tensile load-bearing behavior of further materials. In addition, further analyses will be conducted in ARAMIS<sup>®</sup>, as for example the determination of the strains to analyze the deformation behavior under tensile load.

#### Acknowledgments

Many thanks go to Christian Niejahr from Chair of Thermodynamics of Mobile Energy Conversion Systems, RWTH Aachen University, for the production of the clamps with the CNC mill.

#### 5. References

- [1] Kalthoff M, Gilleßen F, Raupach M, Schmidt S, Kiesewetter-Marko C, Brecher C. Influence of test specimen geometry on the tensile strength behavior of cement-bound concretes. In: 20<sup>th</sup> International Building Materials Conference. Ludwig H-M, Fischer H-B, Eds, Finger-Institute for Building Materials Science, Bauhaus-Universität Weimar. 12-14 September 2018. p.1-1115-1-1122. (in German)
- [2] Neunzig C, Heiermann T, Raupach M. Determination of the uniaxial tensile strength of concrete with a modified test setup. In: Proceedings of the International Conference on Strain-Hardening Cement-Based Composites SHCC4. Mechtcherine V, Slowik V, Kabele P. Eds, Springer Dordrecht. 2018. p.316-323.
- [3] Schubert P, Caballero González A. Tensile strength of autoclaved aerated concrete and adhesive shear strength of thin-layer mortar on autoclaved aerated concrete. Mauerwerk Kalender. Ernst & Sohn.

- 1997;22:629-643. (in German)
- [4] Helbling A, Brühwiler E. A new support for tensile tests with concrete specimen. *Material und Technik*. EMPA Dübendorf. 1987;4:103-107. (in German)
- [5] Kalthoff M, Raupach M, Matschei T. Influence of High Temperature Curing and Surface Humidity on the Tensile Strength of UHPC. *Materials*. 2021;14(4260).
- [6] ASTM C307-18. Standard Test Method for Tensile Strength of Chemical-Resistant Mortar, Grouts, and Monolithic Surfacing. ASTM International. West Conshohocken PA USA. 2018.
- [7] Haufe J, Vollpracht A. Tensile strength of concrete exposed to sulfate attack. *Cement and Concrete Research*. 2019;116:81-88.
- [8] Research Report D01-1185. Interlaboratory Study to Establish Precision Statements for ASTM C307, Test Method for Tensile Strength of Chemical-Resistant Mortar, Grouts, and Monolithic Surfacing. ASTM International. West Conshohocken PA USA. 2018.
- [9] Haufe J, Vollpracht A, Matschei T. Development of a Sulfate Resistance Performance Test for Concrete by Tensile Strength Measurements: Determination of Test Conditions. *Crystals*. 2021;11(1001).
- [10] Okba S H, Nasr E-S A, Helmy A I, Yousef I A-I. Effect of thermal exposure on the mechanical properties of polymer adhesives. *Construction and Building Materials*. 2017;135:490-504.
- [11] Quercia G, Chan D, Luke K. Weibull statistics applied to tensile testing for oil well cement compositions. *Journal of Petroleum Science and Engineering*. 2016;146:536-544.
- [12] Gom. User Guide Setup Testing - ARAMIS Setup Testing for Correlate Pro 2021. 2022.
- [13] TR IH. Technical regulation - Rehabilitation of concrete structures (TR Rehabilitation) - Part 1: Scope and planning of rehabilitation. German Institute for Building Technology (DIBt). 2020. (in German)
- [14] TR IH. Technical regulation - Rehabilitation of concrete structures (TR Rehabilitation) - Part 2: Characteristics of products or systems for rehabilitation and regulations for their use. German Institute for Building Technology (DIBt). 2020. (in German)
- [15] DIN EN 1015-3. Methods of test for mortar for masonry - Part 3: Determination of consistence of fresh mortar (by flow table). German version EN 1015-3:1999+A1:2004+A2:2006. German Institute for Standardisation (DIN). Beuth Verlag GmbH. 2007.
- [16] DIN EN 1015-6. Methods of test for mortar for masonry - Part 6: Determination of bulk density of fresh mortar. German version EN 1015-6:1998+A1:2006. German Institute for Standardisation (DIN). Beuth Verlag GmbH. 2007.
- [17] DIN EN 1015-7. Methods of test for mortar for masonry - Part 7: Determination of air content of fresh mortar. German version EN 1015-7:1998. German Institute for Standardisation (DIN). Beuth Verlag GmbH. 1998.
- [18] DIN EN 196-1. Methods of testing cement - Part 1: Determination of strength. German version EN 196-1:2016. German Institute for Standardisation (DIN). Beuth Verlag GmbH. 2016.
- [19] DIN EN 1015-11. Methods of test for mortar for masonry - Part 11: Determination of flexural and compressive strength of hardened mortar. German version EN 1015-11:2019. German Institute for Standardisation (DIN). Beuth Verlag GmbH. 2020.
- [20] DIN EN 998-2. Specification for mortar for masonry - Part 2: Masonry mortar; German version EN 998-2:2016. German Institute for Standardisation (DIN). Beuth Verlag GmbH. 2017.
- [21] DIN EN 771-4. Specification for masonry units - Part 4: Autoclaved aerated concrete masonry units. German version EN 771-4:2011+A1:2015. German Institute for Standardisation (DIN). Beuth Verlag GmbH. 2015.
- [22] DIN EN 772-1. Methods of test for masonry units - Part 1: Determination of compressive strength. German and English version EN 772-1:2011+A1:2015. German Institute for Standardisation (DIN). Beuth Verlag GmbH. 2015.
- [23] DIN EN 772-13. Methods of test for masonry units - Part 13: Determination of net and gross dry density of masonry units (except for natural stone). German version EN 772-13:2000. German Institute for Standardisation (DIN). Beuth Verlag GmbH. 2000.
- [24] DIN 20000-404. Application of building products in structures - Part 404: Rules for the application of autoclaved aerated concrete masonry units according to DIN EN 771-4:2015-11. German Institute for Standardisation (DIN). Beuth Verlag GmbH. 2018.
- [25] Razali N M, Wah Y B. Power comparisons of shapiro-wilk, kolmogorov-smirnov, lilliefors and anderson-darling tests. *Journal of statistical modeling and analytics*. 2011;2(1):21-33.
- [26] Benning W. *Statistics in geodesy, geoinformation and civil engineering*. Wichmann. 2011.



© 2022 by the authors. This work is licensed under a [Creative Commons Attribution 4.0 International License](http://creativecommons.org/licenses/by/4.0/) (http://creativecommons.org/licenses/by/4.0/). Authors retain copyright of their work, with first publication rights granted to Tech Reviews Ltd.